XII International Conference on Textile Composites and Inflatable Structures
STRUCTURAL MEMBRANES 2025
R. Wüchner, A. K. Goldbach, R. Rossi and C. Lázaro (Eds)

AN OPTIMIZATION-BASED APPROACH TO SHELL MORPHING

L. Mariani[*†], V. Varano[‡], S. Gabriele[‡], L. Greco[†] and M. Cuomo[†]

[*†] University of Catania
Department of Civil Engineering and Architecture - Via Santa Sofia, 64 - 95123 Catania, Italy
e-mail: lucia.mariani@phd.unict.it, leopoldo.greco@unict.it, massimo.cuomo@unict.it
web page: https://www.dicar.unict.it/

[‡] University of Roma Tre
Department of Architecture - Via Aldo Manuzio, 68L - 00153 Rome, Italy
e-mail: valerio.varano@uniroma3.it, stefano.gabriele@uniroma3.it
web page: https://architettura.uniroma3.it/

Key words: shell morphing, optimization, anelastic distortions

Summary. Morphing of continuum bodies offers innovative strategies for shape optimization and structural adaptation in lightweight shell structures. A key challenge in shell morphing is achieving shape transitions in the absence of external forces while ensuring deformation efficiency and optimizing internal stresses.

In previous studies, we explored shape transformations by prescribing non-uniform but isotropic strain fields, achieved through local metric changes to a flat reference domain. This approach leads to the generation of various smooth forms that satisfy a constant curvature requirement. However, when the prescribed metric is not compatible, achieving the desired target configuration becomes inherently infeasible. To address such cases, this study introduces an optimization-based approach leveraging the Comsol Multiphysics' optimization tool. Rather than directly imposing a target metric, which may be geometrically incompatible, we define a target shape and seek the closest achievable final configuration. The optimization process minimizes the distance, measured in terms of displacements or curvature, between the target and the current configuration by optimizing the parameters of an assigned anelastic distortion field involved in the transformation process. This strategy ensures that the final shell placement closely approximates the target form. By embedding this method within the nonlinear shell morphing framework, we extend previous analyses to scenarios where direct metric assignment fails.

This research addresses the growing need for adaptable structures capable of responding to environmental changes, focusing on the precise manipulation of intrinsic geometric properties of the shape. The results provide deeper insights into the role of optimization in controlling shell configurations, with potential applications in architectural and engineering design, where geometric constraints impose fundamental limitations on form-finding and manufacturability.

1 INTRODUCTION

The concept of shape morphing refers to the capability of a structure to perform prescribed geometric transformations by modifying its intrinsic properties rather than being driven by external forces. Within the framework of shell theory and continuum mechanics, this paradigm has become increasingly relevant for the design of lightweight, adaptive, and efficient structural systems. By exploiting intrinsic morphing strategies, shells can dynamically adapt to functional or environmental changes, enabling deployable and bio-inspired configurations[1].

Recent studies have investigated anelastic distortion fields, introduced as local variations of the metric tensor, which induce deformations that inherently activate both membrane and bending mechanisms, enabling complex geometries without external loads[2;3;4]. In contrast to force-driven approaches, this perspective focuses on geometric prescription, offering a rigorous framework for shape design and structural adaptation.

However, when the prescribed metric is intrinsically inconsistent with an embedding in Euclidean space, residual strains develop, preventing the exact realization of the intended geometry. To address this incompatibility, the present work adopts an optimization-based approach that prescribes a target shape and identifies the distortion field leading to the closest realizable configuration. The problem is formulated as the minimization of an objective functional measuring the geometric deviation between the target and current configurations.

The proposed methodology is first validated through a two-dimensional benchmark addressing the morphing from a flat disk to a spherical surface with constant curvature, and subsequently extended to a higher-order case confirming robustness under variable metric and curvature fields. This study advances the control of shape transitions and deformation efficiency within the nonlinear shell morphing framework, contributing to the design of adaptive and lightweight structures capable of achieving prescribed transformations even under intrinsic geometric incompatibility.

2 THEORETICAL FRAMEWORK

The morphing of thin shells is governed by two intrinsic geometric quantities: the metric tensor, controlling in-plane deformations, and the curvature tensor, associated with out-of-plane effects. Prescribing variations of these quantities enables shape transitions without external loads, consistent with the principles of differential geometry and nonlinear shell mechanics[5].

Within this framework, the shell is modeled as a thin manifold embedded in Euclidean space, with the mid-surface containing the essential geometric and mechanical information. The *target shape* is the geometry to be attained, defined by its intrinsic properties, while the *current shape* is the configuration resulting from the anelastic distortion applied to the reference domain. Since prescribed metrics often cannot be embedded without residual strains, the two shapes generally differ, and the problem is formulated as an optimization task to identify the distortion field yielding the feasible configuration closest to the target.

A simple one-dimensional analogy clarifies this concept. Consider a clamped beam of length L and a circular arc spanning the same chord. The clamped ends enforce horizontal tangents, while the arc requires vertical ones, introducing geometric incompatibility. The task is to determine a distortion field that satisfies the constraints while approximating the target arc (Figure 1).

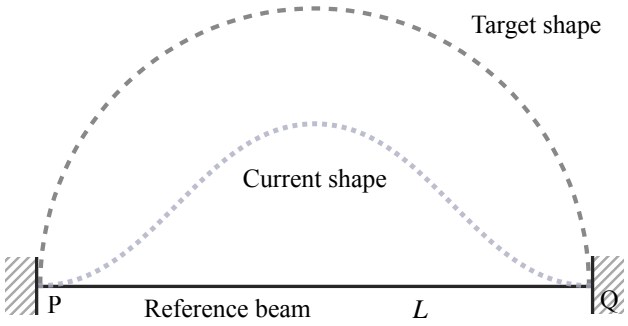

Figure 1: One-dimensional problem setting. The dashed black curve illustrates the target arc, spanning the same length as the clamped beam but requiring boundary tangents incompatible with the imposed constraints. The dotted grey curve depicts a feasible configuration that satisfies the clamped conditions while approximating the target geometry.

2.1 Geometrical setting

We consider a shell-like body defined with respect to an orthonormal frame $\{0; \mathbf{c}_1, \mathbf{c}_2, \mathbf{c}_3\}$ embedded in the Euclidean space $\mathcal{E}^6$. The shell domain is modeled as a flat three-dimensional region $\mathcal{S} = Z \times H$, where $Z \in \mathrm{span}(\mathbf{c}_1, \mathbf{c}_2)$ denotes the planar mid-surface and $H \in \mathrm{span}(\mathbf{c}_3)$ the thickness direction. A thin-shell regime is assumed, with surface extent largely prevailing over thickness, namely $\sqrt{\mathrm{area}(Z)}/H \gg 1$. Each material point of $\mathcal{S}$ is identified by coordinates (x, y, ζ). Although geometrically three-dimensional, the mechanics is effectively two-dimensional: in-plane behavior dominates, while thickness effects are represented by a linear offset of the mid-surface along the unit normal $\mathbf{n}$ scaled by ζ. The deformation is defined by the mapping:

$$\begin{aligned} f &: \mathcal{S} \mapsto \mathcal{E}, \\ \text{with } \; f(x, y, \zeta) &= \hat{f}(x, y) + \zeta \mathbf{n}(x, y). \end{aligned} \tag{1}$$

Here, $\hat{f}(x, y)$ describes the mid-surface placement, $\mathbf{n}(x, y)$ is the unit normal and the parameter ζ provides a first-order representation of thickness effects.

Let $\bar{\mathcal{B}}$ be the reference configuration and $\mathcal{B}$ the deformed one; the mapping f connects the two:

$$f : \bar{\mathcal{B}} \mapsto \mathcal{E}. \tag{2}$$

The deformation gradient $\mathbf{F} = \nabla f$ specifies how material line elements are carried into the ambient space. To represent intrinsic modifications, an anelastic distortion $\mathbf{F}_a$ is introduced, which generally is not the gradient of a mapping. The residual elastic part needed to realize the configuration is then related by:

$$\mathbf{F}_e = \mathbf{F}\mathbf{F}_a^{-1}. \tag{3}$$

Here, $\mathbf{F}_e$ denotes the elastic distortion required to embed the body into the deformed configuration. The three mappings $\mathbf{F}$, $\mathbf{F}_a$, and $\mathbf{F}_e$ lead to the definition of the associated metric tensors:

$$\begin{aligned} \mathbf{C} &= \mathbf{F}^\top \mathbf{F}, \quad \text{the current metric, determined by } \mathbf{F}, \\ \mathbf{C}_a &= \mathbf{F}_a^\top \mathbf{F}_a, \quad \text{the anelastic metric, determined by } \mathbf{F}_a, \\ \mathbf{C}_e &= \mathbf{F}_e^\top \mathbf{F}_e = \mathbf{F}_a^{-\top} \mathbf{C} \mathbf{F}_a^{-1}, \quad \text{the elastic metric, determined by } \mathbf{F_e}. \end{aligned} \tag{4}$$

Accordingly, $\mathbf{C}$ encodes the realized configuration, $\mathbf{C}_a$ the prescribed intrinsic metric, and $\mathbf{C}_e$ the residual strain accomodating the distortion in Euclidean space.

Under the thin-shell hypothesis, the three-dimensional description admits a two-dimensional reduction. From the mapping above, the distortion $\mathbf{F}_a$ can be expressed via the tangent vectors $\mathbf{a}_{a1}, \mathbf{a}_{a2}$ of the mid-surface and its normal $\mathbf{n}_a$, with thickness dependence through ζ:

$$|\mathbf{F}_a| = \left[\mathbf{a}_{a1} \mid \mathbf{a}_{a2} \mid \mathbf{n}_a\right] + \zeta \left[\mathbf{n}_{a,1} \mid \mathbf{n}_{a,2} \mid 0\right]. \tag{5}$$

The associated metric tensor expands as:

$$\mathbf{C}_a = \mathbf{F}_a^\top \mathbf{F}_a = \mathbf{U}_a^2 = \mathbf{A}_a + 2\,\zeta \mathbf{B}_a + 0(\zeta), \tag{6}$$

where $\mathbf{A}_a$ is the first fundamental form (in-plane stretching) and $\mathbf{B}_a$ is the second fundamental form (curvature contribution). Higher-order terms in ζ are negligible for thin shells, so the reduced two-dimensional formulation captures the essential geometric–mechanical content while streamlining the analysis of morphing driven by intrinsic distortions.

2.2 Variational formulation

The introduction of anelastic distortions alters the intrinsic geometry of the shell, making it possible to induce shape changes in the absence of external loads. If the imposed distortion field is consistent with compatibility conditions and boundary constraints, the resulting geometry can develop naturally; otherwise, incompatibilities arise, and the structure accommodates them by storing elastic energy, since the body cannot realize the desired shape as a valid embedding in Euclidean space.

Within an energetic formulation, the problem is recast as the minimization of the elastic energy, which quantifies the gap between the realized *current metric* and the imposed *anelastic metric*. For elastic continua, the energy density ψ is expressed as the sum of membrane and bending contributions

$$\psi = (\psi_m(\mathbf{E}_{e0}) + \psi_b(\mathbf{E}_{e1}))\, J_a, \tag{7}$$

where $J_a = \sqrt{\det \mathbf{A}_a} = \det \mathbf{U}_a$ quantifies the relative area change between the distorted and the reference area elements. The membrane and bending parts read:

$$\begin{aligned} \psi_m(\mathbf{E}_{e0}) &= \mu_1 \mathrm{tr}(\mathbf{E}_{e0})^2 + \mu_2 \mathrm{tr}(\mathbf{E}_{e0}^2), \\ \psi_b(\mathbf{E}_{e1}) &= b_1 \mathrm{tr}(\mathbf{E}_{e1})^2 + b_2 \mathrm{tr}(\mathbf{E}_{e1}^2). \end{aligned} \tag{8}$$

The strain measures $\mathbf{E}_{e0}$ and $\mathbf{E}_{e1}$ depend on the mismatch between the fundamental forms of the current $(\mathbf{A}, \mathbf{B})$ and the anelastic $(\mathbf{A}_a, \mathbf{B}_a)$ configurations:

$$\begin{aligned} \mathbf{E}_{e0} &= \frac{1}{2}\mathbf{U}_{a0}^{-1}(\mathbf{A} - \mathbf{A}_a)\mathbf{U}_{a0}^{-1}, \\ \mathbf{E}_{e1} &= \mathbf{U}_{a0}^{-1}(\mathbf{B} - \mathbf{B}_a - \mathrm{sym}((\mathbf{A} - \mathbf{A}_a)\mathbf{U}_{a0}^{-1}\mathbf{U}_{a1}))\mathbf{U}_{a0}^{-1}. \end{aligned} \tag{9}$$

The stretch tensors $\mathbf{U}_{a0}$ and $\mathbf{U}_{a1}$ associated with the anelastic assignments, are coupled as:

$$\mathbf{U}_{a0} = \sqrt{\mathbf{A}_a}\,, \quad \mathbf{U}_{a1} = \frac{1}{\mathrm{tr}(\mathbf{U}_{a0})}(\mathbf{B}_a + \det(\mathbf{U}_{a0})\mathbf{U}_{a0}^{-1}\mathbf{B}_a\mathbf{U}_{a0}^{-1}). \tag{10}$$

These relations establish the link between the surface geometry and the elastic energy stored as a consequence of anelastic distortions.

The present formulation lays the groundwork for the optimization strategy presented in Section 3.2, aimed at identifying the optimal distortion field that minimizes the residual elastic energy and yields the most consistent configuration with the prescribed target.

3 VALIDATION BENCHMARK

The proposed framework is validated through the disk-to-sphere benchmark, a paradigmatic test case in morphing shell mechanics, as it involves a target surface with constant Gaussian curvature. The problem consists in transforming a flat circular disk into a spherical cap by prescribing an isotropic anelastic distortion field. This configuration highlights the intrinsic geometric incompatibility between planar and curved surfaces, providing an ideal reference case to assess the effectiveness of the proposed approach.

The problem is formulated as a shape optimization task, where the objective functional quantifies the geometric deviation between the realized configuration and the prescribed spherical target. The optimization algorithm iteratively updates the distortion parameters to minimize this deviation, ensuring both geometric and mechanical consistency.

3.1 Morphing setting

The morphing strategy relies on prescribing an anelastic distortion field defined by the first fundamental form $\mathbf{A}_a$, which governs the local stretching of the mid-surface. Due to the geometric coupling inherent in the Gauss equation, this assignment implicitly determines a corresponding second fundamental form $\mathbf{B}_a$. Together, $\mathbf{A}_a$ and $\mathbf{B}_a$ control membrane and bending responses, enabling the transition from a flat reference configuration to a curved equilibrium shape, thus providing a direct geometric route to shape programming through isotropic metric distortions.

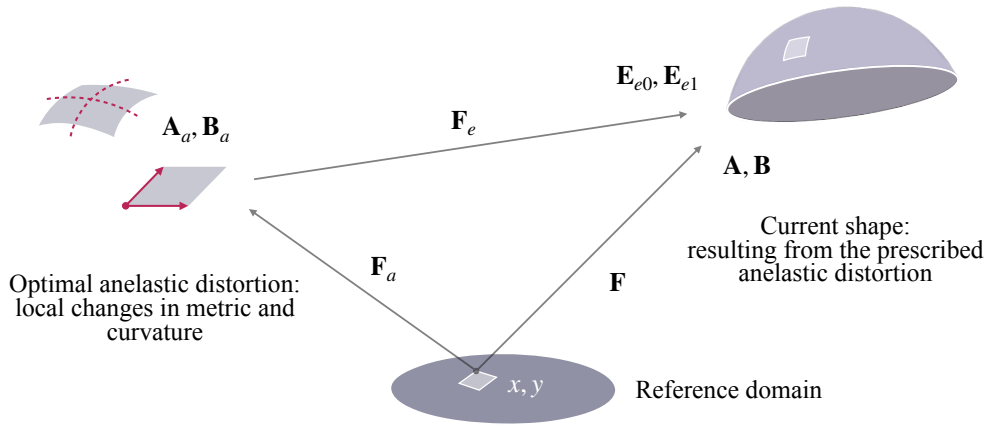

Figure 2: Setting of the morphing model. The flat reference disk (bottom, centre) is modified by prescribing anelastic distortions through changes in the fundamental forms $\mathbf{A}_a$ and $\mathbf{B}_a$. The resulting configuration (top, right) represents the equilibrium state that minimizes the elastic-energy gap between the target and realized metrics.

The disk's ability to reach the target geometry depends on the compatibility of the prescribed distortion with boundary and geometric constraints. When full compatibility is not achieved, internal stresses develop and the system settles into the equilibrium configuration that minimizes residual elastic energy, as discussed in Section 2.2. The optimal distortion corresponds to the parameter set minimizing the geometric distance, expressed in terms of displacement, between the current and target configurations, thus defining the efficiency of the morphing process.

3.2 Optimization problem statement

The optimization procedure aims to identify the parameters of the anelastic distortion that minimize the geometric deviation between the target and the current configurations

The process is implemented in COMSOL Multiphysics through the Nelder-Mead simplex algorithm[7], which iteratively updates the distortion parameters until convergence of the objective functional. To this end, the target placement is introduced as the vector

$$\mathrm{P}_t = \begin{pmatrix} \mathrm{P}_{tx} \\ \mathrm{P}_{ty} \\ \mathrm{P}_{tz} \end{pmatrix}, \tag{11}$$

while the current placement is expressed as the sum of the reference spatial coordinates and the displacement field as:

$$\mathrm{P} = \begin{pmatrix} x \\ y \\ z \end{pmatrix} + \begin{pmatrix} u_1 \\ u_2 \\ u_3 \end{pmatrix}. \tag{12}$$

The objective functional is defined as the integral over the shell domain Ω of the squared distance between the target and current placements, thereby quantifying the geometric discrepancy between the realized configuration and the prescribed target:

$$\Phi = \int_\Omega \left[\big(\mathrm{P}_{tx} - (x + u_1)\big)^2 + \big(\mathrm{P}_{ty} - (y + u_2)\big)^2 + \big(\mathrm{P}_{tz} - (z + u_3)\big)^2 \right] dA. \tag{13}$$

The current geometry and the corresponding displacement field result from the imposed anelastic distortion, encoded in the fundamental forms $\mathbf{A}_a$, $\mathbf{B}_a$. The distortion is described by a parametric isotropic function λ_a, characterized by a finite set of coefficients tuned to minimize the objective functional while ensuring consistency with the governing geometric and mechanical conditions.

3.3 Analytical characterization of the distortion field

In the validation benchmark, the target is a spherical surface characterized by constant Gaussian curvature. The anelastic metric is prescribed through the first fundamental form $\mathbf{A}_{\lambda_a}$, defined by a radially dependent isotropic function $\lambda_a(r)$ which encodes the distortion to be optimized. The anelastic metric $\mathbf{A}_{\lambda_a}$ is formulated as an isotropic tensor expressed in polynomial form.

The isotropy assumption reflects actuation mechanisms that induce uniform in-plane metric variations along both principal directions, while the polynomial representation provides sufficient flexibility to approximate the spherical target using a limited set of optimization parameters.

Accordingly, it can be written as

$$\mathbf{A}_{\lambda_a} = \lambda_a(r)\,\mathbf{I} = \begin{pmatrix} 1+\mu\lambda_a(r) & 0 \\ 0 & 1+\mu\lambda_a(r) \end{pmatrix}, \tag{14}$$

where $r = \sqrt{x^2+y^2}$ is the disk's radial distance and μ is the continuation parameter, ranging in $\mu \in [0,1]$. The continuation parameter controls the gradual application of the distortion: at $\mu = 0$, the disk remains undeformed, while at $\mu = 1$, the complete distortion is applied.

Assuming $\bar{\lambda}_a(r)$ to be an isotropic metric function, its general form can be expressed as a polynomial expansion in the radial coordinate r

$$\bar{\lambda}_a(r) = \lambda_0 + \lambda_1 r + \lambda_2 r^2 + \cdots + \lambda_n r^n, \tag{15}$$

where n is the expansion order and $\lambda_0, \lambda_1, \ldots, \lambda_n$ is the set of coefficients to be optimized.

In the validation case, $\lambda_{a0}(r)$ is represented by an even-order polynomial expansion, truncated at the second degree to approximate the spherical target with a reduced number of parameters:

$$\lambda_{a0}(r) = \lambda_0 + \lambda_2 r^2. \tag{16}$$

The first fundamental form $\mathbf{A}_{\lambda_{a0}}$ associated with $\lambda_{a0}(r)$ therefore becomes:

$$\mathbf{A}_{\lambda_{a0}} = \lambda_{a0}(r)\,\mathbf{I} = \begin{pmatrix} 1+\mu(\lambda_0+\lambda_2 r^2) & 0 \\ 0 & 1+\mu(\lambda_0+\lambda_2 r^2) \end{pmatrix}. \tag{17}$$

According to Gauss' Theorema Egregium, the Gaussian curvature $\mathbf{k}_{\lambda_{a0}}$ can be fully expressed in terms of $\mathbf{A}_{\lambda_{a0}}$ and its derivatives. By using Brioschi's formula, one obtains:

$$\mathbf{k}_{\lambda_{a0}} = -\frac{2\mu\lambda_2(1+\mu\lambda_0)}{(1+\mu\lambda_0+\mu\lambda_2 r^2)^3}. \tag{18}$$

Finally, the second fundamental form $\mathbf{B}_{\lambda_{a0}}$ is determined by enforcing the general compatibility condition linking the two fundamental forms:

$$\begin{aligned} \mathbf{k}_{\lambda_a}\,\mathbf{I} &= \mathbf{B}_{\lambda_a}\,\mathbf{A}_{\lambda_a}^{-1}, \\ \mathbf{B}_{\lambda_a} &= \mathbf{k}_{\lambda_a}\,\mathbf{A}_{\lambda_a}. \end{aligned} \tag{19}$$

This framework provides a rigorous description of the disk-to-sphere morphing transition: the isotropic distortion $\lambda_{a0}(r)$ drives both the metric and the curvature of the surface, while the optimization process calibrates the coefficients λ_0, λ_2 to obtain the closest feasible approximation of the spherical target. The same isotropic metric framework will serve as the foundation for the higher-order morphing case presented in Section 5.

4 NUMERICAL FRAMEWORK

The proposed morphing model has been numerically implemented in COMSOL Multiphysics, combining nonlinear finite element analysis and parametric optimization. The shell is modeled as a two-dimensional manifold embedded in three-dimensional space, where the deformation is expressed through variations of the fundamental forms capturing both in-plane and out-of-plane effects. The governing equations are expressed in weak form, allowing accurate discretization of the mid-surface domain through standard interpolation functions for the displacement field.

The anelastic distortion field is introduced by prescribing a parameterized representation of the fundamental forms, as developed in the previous Subsection 3.3. The optimization iteratively updates the coefficients λ_0 and λ_2 of the isotropic radial distortion $\lambda_{a0}(r)$ to minimize the geometric deviation between the computed configuration and the spherical target. Through this computational procedure, morphologies otherwise inaccessible due to geometric incompatibility can be approximated with accuracy, demonstrating how the coupling between nonlinear metric-based shell modeling and numerical optimization methods enables controlled transitions from flat to curved geometries.

4.1 Target geometry setup

In the validation benchmark, the target surface is a spherical cap characterized by constant Gaussian curvature, serving as a canonical reference for assessing the effectiveness of the proposed morphing strategy. Its placement is described through a cartesian parametrization of the spherical surface (Figure 3):

$$\mathrm{P}_{\mathrm{t}_0} = \left(x,\ y,\ \sqrt{R^2 - r^2}\right). \tag{20}$$

Here, R is the sphere radius and $r = \sqrt{x^2 + y^2}$ denotes the radial distance of the reference disk. This parametrization directly links the flat domain to the spherical surface, however it produces an anisotropic metric distribution: surface elements undergo non-uniform stretching, and coordinate lines lose orthogonality. The resulting mismatch between the isotropic distortion field and the anisotropic target metric makes the disk-to-sphere configuration a significant validation test.

4.2 Optimization results

The overall optimization history for the disk-to-sphere benchmark is summarized in Table 1. The table reports the evolution of the parameters λ_0 and λ_2, defining the isotropic distortion function $\lambda_{a0}(r)$, together with the corresponding values of the objective functional Φ_0, evaluated from the integral definition in (13), and the continuation parameter μ introduced in (14), which governs the gradual application of the imposed distortion. The functional Φ_0 measures the geometric discrepancy between the target and current configurations and thus provides a direct indication of convergence. Its progressive reduction through the iterations confirms the effective minimization of the distance between the realized and the prescribed geometries.

At convergence, the optimization yields the following optimal anelastic distortion:

$$\lambda_{a0}(r) = 0.45 - 1.80r^2. \tag{21}$$

Table 1: Low-order polynomial: selected iteration of the optimization process.

λ_0	λ_2	Φ_0	μ
0.500	1.999	0.178	0.740
0.500	2.000	0.178	0.740
0.500	1.999	0.178	0.740
0.513	1.984	0.209	0.730
1.000	1.000	0.309	0.610
0.700	1.000	0.289	0.640
1.000	0.700	0.610	0.250
0.450	1.800	0.332	0.590

These results confirm that, even under the geometric incompatibility between the isotropic nature of the assigned distortion field and the anisotropic distribution of the target representation, the optimization procedure effectively reduces the discrepancy with the spherical target, providing a feasible realization of the disk-to-sphere transition (Figure 4).

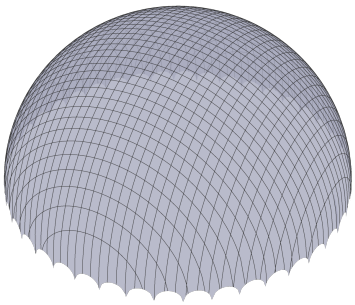

Figure 3: Target placement $\mathrm{P}_{\mathrm{t}_0}$: anisotropic Cartesian parametrization of the sphere.

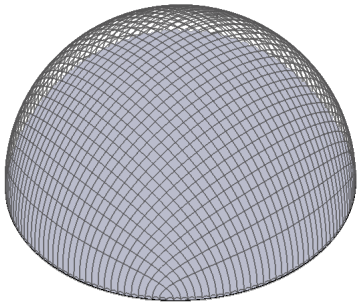

Figure 4: Optimized configuration induced by the prescribed anelastic distortion $\lambda_{a0}(r)$.

5 EXTENDED MORPHING CASE

To further validate the proposed framework, a second benchmark is introduced, involving a target geometry characterized by non-uniform Gaussian curvature. Unlike the disk-to-sphere transition, where the curvature is constant, this case is based on an analytical surface generated by a higher-order radial polynomial. The objective is to assess the capability of the morphing strategy to reproduce geometries with spatially varying intrinsic curvature while preserving isotropy in the prescribed distortion field.

In this setting, the anelastic distortion is described by an isotropic function $\lambda_{a1}(r)$, expressed as an eighth-order polynomial of the radial coordinate r, which defines the radial distribution of in-plane stretching that drives the morphing process toward the desired target configuration.

The anelastic polynomial assignment is expressed as

$$\lambda_{a1}(r) = \sum_{i=0}^{4} \lambda_{2i}\, r^{2i}, \tag{22}$$

where the coefficients λ_{2i} $(i = 0, 1, 2, 3, 4)$ is the set of parameters to be optimized. The associated first fundamental form $\mathbf{A}_{\lambda_{a1}}$ reads:

$$\mathbf{A}_{\lambda_{a1}} = \begin{pmatrix} 1 + \mu \left(\sum_{i=0}^{4} \lambda_{2i}\, r^{2i} \right) & 0 \\ 0 & 1 + \mu \left(\sum_{i=0}^{4} \lambda_{2i}\, r^{2i} \right) \end{pmatrix}. \tag{23}$$

The second fundamental form $\mathbf{B}_{\lambda_{a1}}$ follows from the compatibility relation in (19). By applying Brioschi's formulation to the eighth-order polynomial distortion, the Gaussian curvature $\mathbf{k}_{\lambda_{a1}}$ can be expressed as a function of the metric coefficients, conveniently written in compact form as

$$\mathbf{k}_{\lambda_{a1}}(r) = -\,2\mu\, \frac{\mathrm{F}(\lambda_{2i},\, r^{2i},\, \mu)}{1 + \left(\mu\, \mathrm{G}(\lambda_{2i},\, r^{2i})\right)^3}, \tag{24}$$

where $\mathrm{F}(\lambda_{2i},\, r^{2i},\, \mu)$ and $\mathrm{G}(\lambda_{2i},\, r^{2i})$ represent the polynomial functions collecting the contributions of the distortion coefficients up to the eighth order.

The analytical target surface considered in this benchmark is governed by a higher-order polynomial (Figure 5) and its placement is represented by the following function:

$$\mathrm{P}_{\mathrm{t}_1} = \left(x,\; y,\; \frac{7}{10} - \frac{13}{20} r^2 + \frac{11}{10} r^4 - \frac{7}{5} r^6 + \frac{1}{4} r^8 \right). \tag{25}$$

In this configuration, characterized by a spatially varying Gaussian curvature, the coefficients λ_{2i} govern the radial distribution of curvature, ensuring a smooth transition between the central and peripheral regions of the disk.

The optimization problem follows the same formulation adopted in the previous benchmark, aiming to identify the set of coefficients λ_{2i} that minimize the geometric deviation between the realized and target configurations. The iterative evolution of the parameters λ_{2i}, along with the corresponding values of the objective functional Φ_1 evaluated in (13) and the continuation parameter μ introduced in (14), is summarized in Table 2.

At convergence, the optimization yields the following optimal polynomial distortion:

$$\lambda_{a1}(r) = 0.13 + 0.70 r^2 + 1.07 r^4 + 0.94 r^6 + 1.65 r^8. \tag{26}$$

Table 2: High-order polynomial: selected iteration of the optimization process.

λ_0	λ_2	λ_4	λ_6	λ_8	Φ_1	μ
1.000	1.000	1.000	1.000	1.000	0.150	0.350
0.700	1.000	1.000	1.000	1.000	0.100	0.490
1.000	0.700	1.000	1.000	1.000	0.132	0.390
1.000	1.000	1.000	0.700	1.000	0.226	0.300
0.490	0.778	1.032	1.064	1.281	0.080	0.520
0.295	0.727	1.108	0.946	1.481	0.056	0.620
0.130	0.673	1.096	0.933	1.719	0.031	0.910
0.127	0.702	1.065	0.943	1.645	0.027	0.960

Compared to the validation benchmark, this extended case highlights the increased flexibility of the proposed framework. The inclusion of higher-order polynomial terms enhances control over the geometric response and enables smoother curvature variations, yielding a closer yet not exact approximation of the target shape (Figure 6).

Some discrepancies remain in areas of pronounced curvature change, where the isotropic distortion field cannot fully capture the metric's spatial variability. However, the resulting configuration is coherent and mechanically consistent, confirming the reliability of the approach under variable curvature conditions. To address these limitations, future work will extend the optimization to curvature-related quantities for a more comprehensive description of the morphing process.

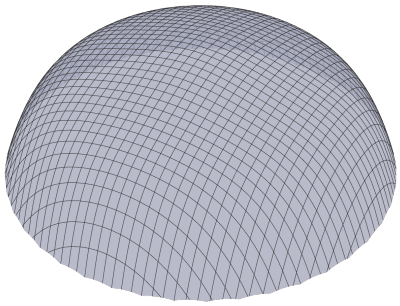

Figure 5: Target placement $\mathrm{P}_{\mathrm{t}_1}$ described by the eighth-order polynomial function.

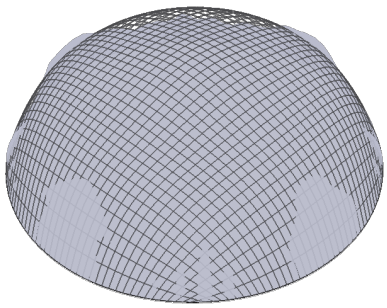

Figure 6: Optimized configuration induced by the prescribed anelastic distortion $\lambda_{a1}(r)$.

6 CONCLUSIONS

This study presents an optimization-based strategy for morphing thin shells through prescribed anelastic distortions, combining a variational formulation, finite element implementation, and gradient-free optimization. The approach aims to identify the closest feasible configuration to a target shape by tuning a low-dimensional distortion field, thereby enabling controlled and computationally efficient morphing under intrinsic geometric incompatibility.

The framework was validated through two benchmarks. The disk-to-sphere transition, consid-

ered as a canonical test, demonstrated the capability of the method to reconcile a target parametrization with anisotropic features through an isotropic distortion assignment, effectively bridging the mismatch between planar and curved geometries. The extended case, based on an eighth-order isotropic polynomial, introduced additional degrees of freedom to represent variable curvature. The obtained configuration reproduced smooth curvature variations and provided a valid result, although localized regions with sharp curvature gradients remain difficult to capture and will require dedicated analysis in future developments.

The results define a compact and stable formulation that effectively links geometric prescription and mechanical response through a reduced set of distortion parameters, proving suitable for inverse morphing problems constrained by geometry, such as architectural and lightweight deployable surfaces. While effective, the formulation remains limited by the isotropy assumption of the distortion field, which restricts the range of target geometries. Future work will extend the framework toward anisotropic and direction-dependent distortions, possibly introducing multi-objective optimization to improve localized curvature control.

In summary, the proposed formulation offers a reliable and scalable route to shape programming of shells under geometric incompatibility, enabling accurate and efficient morphing across constant and variable curvature targets, and paving the way for future integration with actuation or experimental validation toward fabrication-oriented adaptive systems.

REFERENCES

[1] S. Adriaenssens, P. Block, D. Veenendaal and C. Williams, Shell structures for architecture: Form finding and optimization, Routledge, 2014.

[2] G.R. Argento, S. Gabriele, L. Teresi and V. Varano, “Target metric and Shell Shaping”, Curved and Layered Structures, 8 (1), pp. 13–25, 2021.

[3] L. Teresi, F. Milicchio, S. Gabriele, P. Piras and V. Varano, “Shape deformation from metric’s transport”, International Journal of Non-Linear Mechanics, 119, 103326, 2020.

[4] P. Nardinocchi, L. Teresi and V. Varano, “The elastic metric: A review of elasticity with large distortions”, International Journal of Non-Linear Mechanics, 56, pp. 34–42, 2013.

[5] P. G. Ciarlet, An introduction to differential geometry with applications to elasticity, Springer, Hong Kong, 2005.

[6] W. Koiter, “On the nonlinear theory of thin elastic shells”, in Proceedings of the Koninklijke Nederlandse Akademie van Wetenschappen, Series B: Physical Sciences, vol. 69, 1966, pp. 1–54.

[7] J.A. Nelder and R. Mead, “A Simplex Method for Function Minimization”, The Computer Journal, 7 (4), pp. 308–313, 1965.

[8] M.P. do Carmo, Differential Geometry of Curves and Surfaces, Dover Publications, Mineola, New York, 2016.